

results in the production of two equivalents of alkalinity per mole.

14. Sulfate is routinely accurately measured on ODP cruises. In contrast, because sediments outgas as cores are brought up through the water column, concentrations of CH₄ in deep-sea porewaters cannot routinely be accurately estimated from ODP CH₄ concentration data (headspace analysis). This quality of the CH₄ data does not preclude using these SO₄²⁻ and CH₄ data (i) to map downhole profiles of relative CH₄ abundance, or (ii), as described in the text, to estimate steady-state rates of sulfate-reducing methane oxidation and (by inference) CH₄ production. The DSDP and ODP shipboard data used for these profiles and maps were edited to remove samples affected by seawater contamination and sites where spot coring, poor core recovery, or intermittent porewater sampling caused large gaps that rendered profiles difficult to interpret. Sites with fewer than three samples in the zone of stable SO₄²⁻ concentrations were excluded from the SO₄²⁻ map. Because we limited our study to the diffusional realm typical of open-ocean sediments, this analysis omitted stratigraphic intervals from downhole SO₄²⁻ and CH₄ records in cases where porewater chemical profiles were unambiguously affected by hydrologic flow or pronounced lithologic breaks, subsurface anhydrite deposits, or sulfate-enriched brines. Sites identified as probably affected by CaSO₄ precipitation in the underlying basement were also deleted from the SO₄²⁻ map.
15. P. N. Froelich *et al.*, *Geochim. Cosmochim. Acta* **43**, 1075 (1979).
16. M. E. Q. Pilson, *An Introduction to the Chemistry of the Sea* (Prentice Hall, Upper Saddle River, NJ, 1998).
17. The one known exception is mud-volcano ODP Site 779 in the western Pacific (32), where CH₄ may be diffusing up into the sediments after being created by the heating of buried organic matter.
18. T. Fenchel, G. M. King, T. H. Blackburn, *Bacterial Biogeochemistry* (Academic Press, San Diego, CA, 1998).
19. G. M. King, *Geomicrobiol. J.* **3**, 275 (1984).
20. The rate of subsurface SO₄²⁻ reduction at steady state is equal to the downward flux of SO₄²⁻ into the sediments. At any given site, the depth-integrated SO₄²⁻ flux into the sediment and the reduction rate of SO₄²⁻ as a function of depth can be estimated from the porewater profile of dissolved SO₄²⁻, porosity, and core-based estimates of effective diffusivity (33). Diffusivity depends on the porosity and tortuosity of the sediment (33).
21. A. J. Spivack *et al.*, *Eos* **81**, F216 (2000).
22. P. Wellsbury *et al.*, *Nature* **388**, 573 (1997).
23. For this study, the top of the subsurface biosphere is defined as 1.5 mbsf. Total subsurface respiration estimates assume SO₄²⁻ + C₆H₁₂O₆ → S²⁻ + 6CO₂ + 6H₂O. For the system where fermentation plus methanogenesis and anaerobic methane oxidation occurs, they assume (i) C₆H₁₂O₆ → 3CH₄ + 3CO₂ and (ii) SO₄²⁻ + CH₄ → S²⁻ + CO₂ + 2H₂O. Flux uncertainties are 2σ estimates derived from standard deviations in the slopes of the sulfate concentration profiles, as well as assumptions of 10% uncertainty in diffusivity and 30% relative uncertainty in porosity. The latter assumptions are based on standard deviations of diffusivity and porosity measurements at representative sites. Photosynthesis estimates are from (34).
24. D. E. Canfield, *Am. J. Sci.* **291**, 177 (1991).
25. C. Niewöhner, C. Hensen, S. Kasten, M. Zabel, H. D. Schultz, *Geochim. Cosmochim. Acta* **62**, 455 (1998).
26. M. Adler, C. Hensen, S. Kasten, H. D. Schultz, *Int. J. Earth Sci.* **88**, 641 (2000).
27. All estimates of cell abundance are acridine orange direct counts from (6, 35). Uncertainties in per-cell reduction rates are 2σ estimates derived from the standard deviations in flux estimates (Table 1) and standard deviations in the cell counts (typically 30 to 40%). Mean SO₄²⁻ reduction per cell is integrated to the greatest depth sampled for cell counts at Site 834 (100 mbsf) and Site 1149 (400 mbsf). Mean SO₄²⁻ reduction per cell at Site 851 is limited to sediments shallower than 150 mbsf, because at greater depths at this site, SO₄²⁻ is introduced by diffusion from the underlying oceanic crust.
28. B. B. Jørgensen, *Geomicrobiol. J.* **1**, 49 (1978).

29. C. Knoblauch, B. B. Jørgensen, J. Harder, *Appl. Environ. Microbiol.* **65**, 4230 (1999).
30. K. Ravensschlag, K. Sahn, C. Knoblauch, B. B. Jørgensen, R. Amann, *Appl. Environ. Microbiol.* **66**, 3592 (2000).
31. Per-cell sulfate reduction rates in pure cultures of sulfate-reducing bacteria are typically about an order of magnitude higher than per-cell rates in natural sulfate-reducing ecosystems because most cells in natural environments are not sulfate reducers. In natural ecosystems where SO₄²⁻ is the terminal electron acceptor, sulfate-reducing bacteria reduce the terminal electron acceptor. Cells that undertake other steps in the ecosystem's collective metabolic pathways need not be sulfate reducers. For example, in the Arctic coastal sediments used to calculate these near-surface per-cell reduction rates, sulfate-reducing bacteria constitute 4 to 16% of enumerated cells and their RNA constitutes 11 to 29% of the prokaryotic RNA (30).

32. P. Fryer, J. A. Pearce, L. B. Stokking, Shipboard Scientific Party, *Proc. ODP Init. Rep.* **125**, 687 (1990).
33. R. A. Berner, *Early Diagenesis: A Theoretical Approach* (Princeton Univ. Press, Princeton, NJ, 1980).
34. M. J. Behrenfeld, P. G. Falkowski, *Limnol. Oceanogr.* **42**, 1 (1997).
35. B. A. Cragg, R. J. Parkes, personal communication.
36. Edited (14) methane and sulfate profile data represented on the maps are available on Science Online at www.sciencemag.org/cgi/content/full/295/5562/2067/DC1.
37. We thank D. C. Smith, A. Teske, B. B. Jørgensen, and three anonymous reviewers for thought-provoking and helpful discussions. Supported by the Joint Oceanographic Institutions U.S. Science Support Program and the NASA Astrobiology Institute. All porewater chemical data were provided by the Ocean Drilling Program.

30 July 2001; accepted 8 February 2002

Demographic Characteristics and Population Dynamical Patterns of Solitary Birds

Bernt-Erik Sæther,^{1*} Steinar Engen,² Erik Matthysen³

In birds and many other animals, there are large interspecific differences in the magnitude of annual variation in population size. Using time-series data on populations of solitary bird species, we found that fluctuations in population size of solitary birds were affected by the deterministic characteristics of the population dynamics as well as the stochastic factors. In species with highly variable populations, annual variation in recruitment was positively related to the return rate of adults between successive breeding seasons. In stable populations, more recruits were found in years with low return rates of breeding adults. This identifies a gradient, associated with the position of the species along a "slow-fast" continuum of life history variation, from highly variable populations with a recruitment-driven demography to stable, strongly density-regulated populations with a survival-restricted demography. These results suggest that patterns in avian population fluctuations can be predicted from a knowledge of life-history characteristics and/or temporal variation in certain demographic traits.

One of the challenges in ecology is to identify characteristics that can be used to predict interspecific differences in patterns of population fluctuations (1). Comparisons covering a wide range of taxa have shown a strong pattern of covariation of life history traits that divide species along a "slow-fast continuum" (2–6). Life history characteristics such as early onset of reproduction, rapid ontogenetic development, and large litter sizes are typical for species at one end of this continuum, whereas species with low reproductive rates, but longer life expectancies, are found at the other end. Several hypotheses have been proposed to explain this covariation among life

history traits, e.g., density-dependent *r-K* selection (3), adaptive life history responses to differences in extrinsic mortality (5), or adaptations to variation in predictability or variability of the habitats (7). Few studies have, however, quantitatively examined how characteristics of the population dynamics are related to the species' position along this continuum of life history variation; an exception was Fowler (8, 9), who showed that the pattern of density regulation was related to the rate of increase per generation. The presence of such patterns will enable characterization of patterns in population fluctuations from knowledge of basic demography or life history characteristics. Here we used data on the fluctuations of solitary bird populations to examine stochastic effects on population fluctuations. This enables us to quantitatively relate patterns in population dynamics to the position of the species along the slow-fast continuum of life history variation.

To examine how interspecific variations in population dynamical characteristics are affect-

¹Department of Zoology, Norwegian University of Science and Technology, N-7491 Trondheim, Norway. ²Department of Mathematical Sciences, Norwegian University of Science and Technology, N-7491 Trondheim, Norway. ³Erik Matthysen, Laboratory of Animal Ecology, Department of Biology, University of Antwerp, B-2610 Antwerp, Belgium.

*To whom correspondence should be addressed. E-mail: bernt-erik.sather@chembio.ntnu.no

ed by the deterministic and the stochastic components of the dynamics, we chose to describe the population fluctuations by the nonlinear theta-logistic model of density regulation (10). This model has relatively well-understood statistical properties (11, 12) and allows us to model the form of density dependence and strength of density regulation at K by varying only one parameter, θ . For small values of θ , the specific growth rate r decreases rapidly with population size at lower densities (Fig. 1A). In contrast, for large values of θ , a large reduction in r occurs when approaching the carrying capacity K . As expected from these relations, variation in θ strongly influences the dynamical characteristics of the population model. For a given environmental stochasticity, large fluctuations in population size are found when θ is small (Fig. 1B), whereas more stable fluctuations occur for

larger values of θ (Fig. 1C). Accordingly, the variance of the stationary distribution of the population size N decreases with increasing θ (Fig. 1D). Furthermore, the theta-logistic model can also describe, by appropriate choices of θ , more commonly used models of density regulation. For instance, for $\theta = 0$, we have a Gompertz density regulation, $\theta = 1$ gives the logistic model, and for $\theta = \infty$, there is no density regulation below K . Thus, by estimating θ , we will be able to represent a wide range of variation in the expected dynamics of populations.

With the use of a data set of long-term population fluctuations of 13 solitary bird species (Table 1, Fig. 2), an examination of the residuals [see (13)] showed that the theta-logistic model could be fitted to the time series quite well, with no significant time delays (lag less than 4) in any of the species. A strong covariation across species was found between the environmental stochasticity and the parameters describing the expected dynamics (14). The logarithm of environmental stochasticity σ_e^2 decreased with θ (Fig. 3A; correlation coefficient = -0.58 , $P = 0.036$, $n = 13$) but increased with the specific population growth rate r_1 (Fig. 3B; correlation coefficient = 0.61 , $P = 0.026$, $n = 13$). This former relation may, however, have been an artifact effect of a negative sampling covariance because there was a small, but negative, correlation (correlation coefficient < -0.23) between the bootstrap replicates of θ and σ_e^2 in all populations. Assuming that $(\ln \sigma_e^2, \theta)$ was binormally distributed among

species, a meta-analysis (15) showed that the best fit to the data turned out to be the degenerate binormal with correlation -1 , indicating that the negative relation in Fig. 3A is not due to a sampling effect. Furthermore, θ increased with adult survival rate (correlation coefficient = 0.60 , $P = 0.029$, $n = 13$). Thus, a strong pattern of covariation is present among the parameters describing the population dynamics of solitary birds; i.e., density regulation starts to act at lower densities (relative to K) in populations with high values of r_1 and σ_e^2 than in populations with smaller values of those two parameters. This is similar to a pattern previously noted in mammals (8, 16), as well as over a wide range of taxa (9), that density regulation occurs at higher relative densities in long-lived species with a low specific growth rate than in species with higher growth rates. We also notice that θ was larger than 7 in several of the species. This suggests that the commonly used assumption in population ecology of vertebrates (17) of a log-linear density regulation ($\theta = 0$) may not always be justified.

There was large interspecific variation in the coefficient of variation (with only the past 15 years of data) in the fluctuations of the populations included in the present study (Fig. 2), from $CV = 0.08$ (CV is coefficient of variation in population size) in the stable Sparrowhawk *Accipiter nisus* population to 0.71 in the Cactus Finch *Geospiza scandens* population (Table 1). Population variability increased with the environmental stochastic-

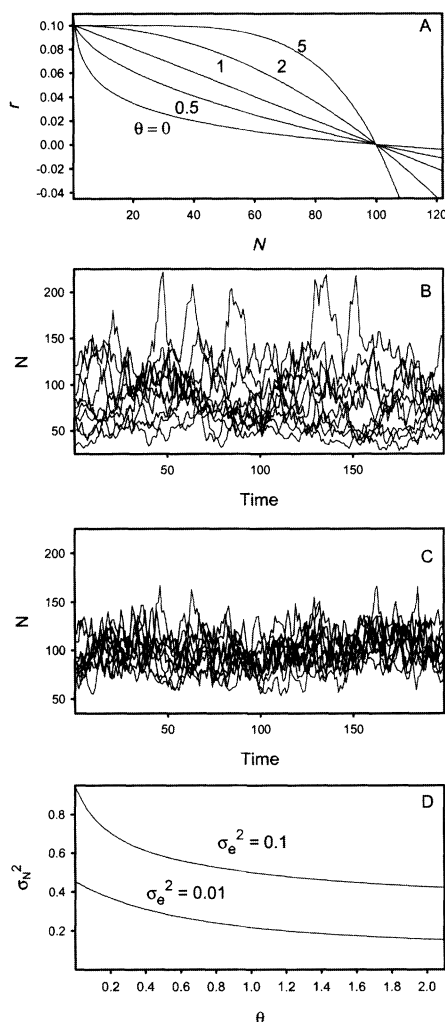


Fig. 1. (A) The relation between the specific growth r and population size N for different θ in the theta-logistic model (14). (B and C) Ten trajectories of the population fluctuations during a period of 200 years in the theta-logistic model for $\theta = 0.1$ (B) and $\theta = 1.5$ (C), assuming that $\sigma_e^2 = 0.01$. (D) The variance in the stationary distribution of population size (σ_N^2) in relation to θ for $\sigma_e^2 = 0.01$ and $\sigma_e^2 = 0.1$.

Table 1. The estimated values (\pm SD) of the parameters describing the dynamics of the bird populations [for sources, see (13)]. CV is the coefficient of variation in population size (calculated during the past 15 years of study), K is the carrying capacity, θ describes the form of the density regulation (11), and σ_e^2 is the environmental stochasticity.

Species	CV	K	θ	σ_e^2
Sparrowhawk	0.08	33.74 ± 0.93	2.57 ± 0.69	0.009 ± 0.011
<i>Accipiter nisus</i>				
White Stork	0.10	45.14 ± 1.84	1.16 ± 0.56	0.006 ± 0.002
<i>Ciconia ciconia</i>				
South Polar Skua	0.15	36.03 ± 15.74	1.78 ± 2.48	0.022 ± 0.025
<i>Catharacta maccormicki</i>				
Mute Swan	0.22	53.85 ± 7.82	1.64 ± 0.74	0.088 ± 0.032
<i>Cygnus olor</i>				
Oystercatcher	0.23	65.72 ± 15.74	1.79 ± 2.48	0.070 ± 0.025
<i>Haematopus ostralegus</i>				
Pied Flycatcher	0.25	286.56 ± 39.68	0.50 ± 0.46	0.034 ± 0.009
<i>Ficedula hypoleuca</i>				
Blue Tit	0.30	22.18 ± 2.02	0.26 ± 0.22	0.068 ± 0.017
<i>Parus caeruleus</i>				
Great Tit	0.21	33.17 ± 2.69	0.44 ± 0.20	0.066 ± 0.016
<i>Parus major</i>				
Nuthatch	0.33	19.43 ± 2.94	0.47 ± 0.37	0.058 ± 0.016
<i>Sitta europaea</i>				
Dipper	0.38	61.72 ± 14.89	0.73 ± 0.42	0.184 ± 0.063
<i>Cinclus cinclus</i>				
Medium Ground Finch	0.54	387.45 ± 79.96	0.59 ± 0.20	0.281 ± 0.100
<i>Geospiza fortis</i>				
Willow Grouse	0.56	125.09 ± 58.22	0.14 ± 1.27	0.190 ± 0.078
<i>Lagopus lagopus</i>				
Cactus Finch	0.71	127.64 ± 46.13	0.37 ± 0.26	0.350 ± 0.134
<i>Geospiza scandens</i>				

REPORTS

ity σ_e^2 (Fig. 3C, Table 1; correlation coefficient = 0.88, $P < 0.001$, $n = 13$) but decreased with θ (Fig. 3D; correlation coefficient = -0.66 , $P = 0.015$, $n = 13$). A partial correlation analysis showed that θ explained a significant proportion of the CV even after accounting for the effect of σ_e^2 (partial correlation = -0.69 , $df = 10$, $P = 0.013$). Thus, the recorded interspecific differences in the variability of the bird populations (Table 1, Fig. 2) are due to differences in the expected dynamics as well as variation in the stochastic effects (18).

In birds, large interspecific variation is found in the mean as well as the variance of most demographic traits (6). How this demographic variation translates into population dynamics is,

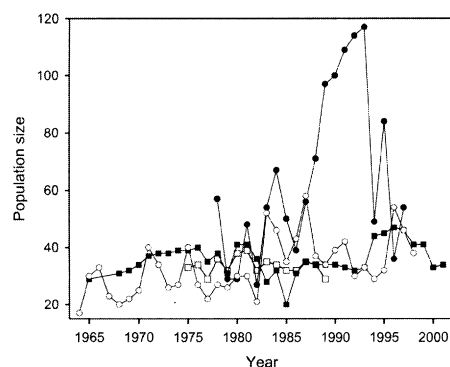


Fig. 2. Population fluctuations in two variable species [Great Tit (○) and Dipper (●)] and two species with smaller coefficients of variation: European Sparrowhawk (■) and South Polar Skua (□). For sources, see (13).

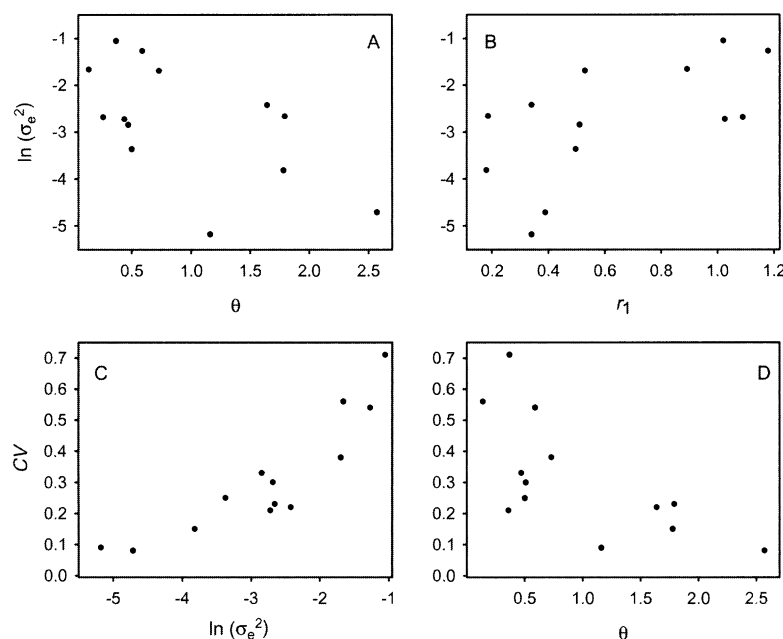


Fig. 3. Interspecific variation in the logarithm of the environmental stochasticity σ_e^2 in relation to the density regulation θ (A) and r_1 , the specific growth rate when the population size $N = 1$ (B), and interspecific variation in the coefficient of variation in population size CV (calculated for the past 15 years of data) in relation to the logarithm of the environmental stochasticity σ_e^2 (C) and the density regulation θ (D). For sources of the data, see (13).

however, poorly understood. Thus, in our final step, we related the described patterns in population dynamics to interspecific differences in demographic processes. We characterized the demography by the correlation coefficient between the annual variation in the number of new recruits and the return rate of adults from one breeding season to the next. This description of recruitment was chosen on the basis of available evidence (19), suggesting that many bird populations are regulated by territorial behavior. In long-lived species, adults may breed in the same territory for several years, and new birds rapidly occupy vacant territories. Thus, the number of new recruits in long-lived territorial species such as the Sparrowhawk (Fig. 4A; correlation coefficient = -0.76 , $P = 0.003$, $n = 13$) and South Polar Skua *Catharacta maccormicki* (correlation coefficient = -0.46 , $P = 0.019$, $n = 26$) was negatively related to the return rate of adults from the previous breeding season. In contrast, in species with lower survival rates, a high turnover of adult birds will occur, in many cases related to variation in environmental conditions or population size during the nonbreeding season, affecting both juveniles and adults (20). Thus, a positive relation was found between annual variation in the number of recruits and the return rate of adult females in short-lived territorial species such as the Great Tit *Parus major* (Fig. 4B; correlation coefficient = 0.66 , $P < 0.001$, $n = 34$) and the Dipper *Cinclus cinclus* (correlation coefficient = 0.59 , $P = 0.008$, $n = 19$). A strong relation was found between this correlation coefficient and the logarithm of θ (Fig. 4C; correlation coefficient = -0.90 , $P =$

0.005 , $n = 7$). As expected from Fig. 3A, a strong relation was also found between this correlation coefficient and σ_e^2 (correlation coefficient = 0.86 , $P = 0.012$, $n = 7$). This shows that a recruitment-driven demography is found in populations with density regulation acting at smaller densities (relative to K) and high environmental stochasticity, whereas a survival-restricted demography is characteristic in populations with strong density regulation around K and small values of σ_e^2 . As a consequence of these relations, CV increased with increasing correlation between annual variation in recruitment and adult return rates (correlation coefficient = 0.75 , $P = 0.0153$, $n = 7$).

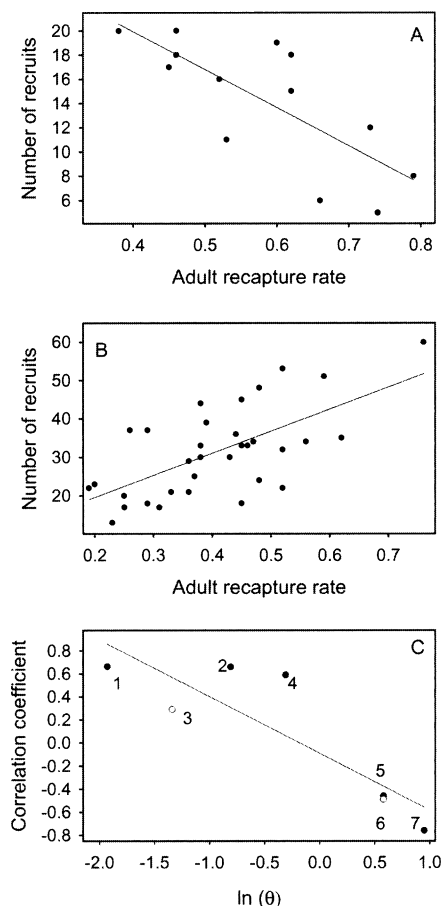


Fig. 4. The relation between annual variation in the number of recruits in relation to the return rate of adults from the previous breeding season (A) in a survival-restricted Sparrowhawk population and (B) in a recruitment-driven Great Tit population. (C) The correlation coefficient between annual variation in the number of recruits and the return rate of adults from the previous breeding season [as illustrated in (A) and (B)] in relation to the density regulation θ in populations of some of the species listed in Table 1. Filled circles denote a significant correlation coefficient, whereas open circles represent an insignificant ($P > 0.05$) relation. The species are as follows: 1, Willow Grouse; 2, Great Tit; 3, Blue Tit; 4, Dipper; 5, South Polar Skua; 6, Oystercatcher; and 7, Sparrowhawk. For sources of the data, see (13).

REPORTS

$$\gamma = r_m \theta = r_1 \theta / (1 - K^{-\theta}),$$

We conclude that differences in population variability were affected by the deterministic characteristics of the population dynamics as well as the stochastic factors (Fig. 3, C and D). These differences were in turn related to the position of the species along slow-fast continuum of life history variation (3, 5, 6) as expressed by r_1 (Fig. 3B). The relative contribution of the parameters describing the expected dynamics and stochastic factors to the population fluctuations is in solitary birds likely to be closely related to the type of demographic process, i.e., whether it is recruitment-driven or survival-restricted (Fig. 4). Fluctuations in the size of recruitment-driven populations are more strongly influenced by environmental stochasticity than survival-restricted populations. Consequently, reliable projections of avian populations will require precise estimates and modeling of stochastic as well as deterministic components of the dynamics. On the other hand, estimating the form of density dependence will be more important for predicting population fluctuations of long-lived species with high values of θ . Reliable estimates of the environmental stochasticity (11) as well as precise estimates of the carrying capacity (21) will require access to long-term time series with small sampling errors (29).

References and Notes

- R. M. May, *Philos. Trans. R. Soc. London* **351**, 1951 (1999).
- R. C. Lewontin, in *The Genetics of Colonizing Species*, H. G. Baker, G. L. Stebbins, Eds. (Academic Press, New York, 1965), pp. 77–91.
- E. R. Pianka, *Am. Nat.* **104**, 592 (1970).
- D. E. L. Promislow, P. H. Harvey, *J. Zool.* **220**, 417 (1990).
- E. L. Charnov, *Life History Invariants* (Oxford Univ. Press, Oxford, 1993).
- B.-E. Sæther, Ø. Bakke, *Ecology* **81**, 642 (2000).
- T. R. E. Southwood, *J. Anim. Ecol.* **46**, 337 (1977).
- C. W. Fowler, *Ecology* **62**, 602 (1981).
- _____, *Evol. Ecol.* **2**, 197 (1988).
- M. E. Gilpin, F. J. Ayala, *Proc. Natl. Acad. Sci. U.S.A.* **70**, 3590 (1973).
- B.-E. Sæther et al., *Am. Nat.* **151**, 441 (1998).
- O. Diserud, S. Engen, *Am. Nat.* **155**, 497 (2000).
- Supplementary material is available on Science Online at www.sciencemag.org/cgi/content/full/295/5562/2070/DC1.
- We based our analyses on time series of populations of solitary bird species that have been censused for 15 or more years with no significant linear trend in population size with time and no population estimate of less than 10 pairs. To reduce the bias in the parameters because of large sampling errors in population estimates, we only included time series that were based on direct nest counts (e.g., hole nesters) or on the presence of a large number of color-ringed individuals. The population parameters were estimated by maximum likelihood methods. We modeled fluctuations in the size of the logarithm of the population fluctuations, $X = \ln N$, where N is the population size at time t . Let $\Delta X = \ln(N + \Delta N) - \ln(N)$ and σ_e^2 be the environmental stochasticity (23). We assume large enough population sizes to ignore any effects of demographic stochasticity. The distribution of ΔX , conditional on N , is assumed to be normal with mean $m(x) = r_m [1 - (N/K)^\theta] \Delta t$ and variance $\sigma_e^2 \Delta t$. Here K is the carrying capacity, r_m is the mean specific growth rate, and θ describes the type of density regulation in the theta-logistic function (10) $m(x)$. The strength of the density regulation at K is then (21)
- where r_1 is the specific growth rate when $N = 1$. Thus, strong density regulation occurs at K when the population growth rate is high and/or for large values of θ . The parameters were estimated by maximum likelihood. The expected change in the logarithm of population size may be written as $E(\Delta X) = r_1 [1 - ((e^{X_0} - 1)/(e^{\theta \ln(K)} - 1))] = \mu(X, K, \theta)$ for $\theta \neq 0$ and $E(\Delta X) = r_1 [1 - (X/\ln K)]$ for $\theta = 0$ (21, 23). The parameters are estimated by maximizing the likelihood function $L(K, \theta, \sigma_e^2) = \prod_{i=1}^n f(X_{i+1} | X_i, K, \theta, \sigma_e^2)$, where $X_0 = K$, and $X_{i+1} = X_i + \Delta X_i$. The function $f(X_{i+1} | X_i, K, \theta, \sigma_e^2)$ is the normal distribution with mean $X_i + \mu(X_i, K, \theta)$ and variance σ_e^2 . The uncertainty in the parameters was determined by simulating repeated data sets from the model, with the maximum likelihood estimates of the parameters, and then calculating bootstrap replicates from each simulation. Reliable estimates of r_1 are often difficult to obtain in stationary time series because the populations most of the time are found fluctuating around K (24). We therefore estimated this parameter by a standard Leslie matrix model (6) using available demographic information. We entered into the model maximum fecundity rate (number of offspring produced to independence per female) and the lowest age specific mortality rate recorded during the study period or in any age class. The estimates of r_1 obtained in this way were in nine bird species (25) closely correlated to bias-corrected values of r_1 obtained from time-series analyses (correlation coefficient = 0.73, $P < 0.05$, $n = 9$).
- We assume that the parameters (θ , $\ln \sigma_e^2$) are binormally distributed among the species and that the estimates of these parameters are approximately binormally distributed for each species with parameters determined by the results of the parametric bootstrapping (14). Each pair of estimates (θ , $\ln \sigma_e^2$) will then have bivariate normal distributions. Estimates of the binormal variation among species are found by maximum likelihood.
- C. W. Fowler, *Curr. Mammol.* **1**, 401 (1987).
- T. Royama, *Analytical Population Dynamics* (Cambridge Univ. Press, Cambridge, 1992).
- A problem in analyses of time series of population fluctuations is that the coefficient of variation increases with the census period (26, 27) because of autocorrelations due to age structure effects, delayed density dependence, or autocorrelation in the environmental noise (28, 29). However, from the diffusion approximation for the theta-logistic model, we can calculate the variance of the stationary distribution (12). If we assume the demographic variance σ_d^2 to be much less than the product of the carrying capacity K and environmental stochasticity σ_e^2 , we can compute the variance of the stationary distribution of population sizes $\sigma_N^2 = K^2 \Gamma[(\alpha + 2)/\Gamma(\alpha + 1)] / \theta^2 \Gamma(\alpha/\theta)$, where $\alpha = 2r_1/\sigma_e^2(1 - K^{-\theta}) - 1$, r_1 is the growth rate when $N = 1$, and Γ denotes the gamma function (12). Thus, σ_N^2 can be used to compare the variability in time series of different lengths. However, in the present data set, a close correlation was found between σ_N^2 and CV (correlation coefficient = 0.94, $P < 0.001$, $n = 13$).
- I. Newton, *Population Limitation in Birds* (Academic Press, San Diego, 1998).
- P. Arcese, J. N. M. Smith, W. M. Hochachka, C. M. Rogers, D. Ludwig, *Ecology* **73**, 805 (1992).
- B.-E. Sæther, S. Engen, R. Lande, P. Arcese, J. N. M. Smith, *Proc. R. Soc. London Ser. B* **267**, 621 (2000).
- R. Lande et al., *Am. Nat.*, in press.
- S. Engen, Ø. Bakke, A. Islam, *Biometrics* **54**, 840 (1998).
- S. Aanes, S. Engen, B.-E. Sæther, T. Willebrand, V. Marström, *Ecol. Appl.*, **12**, 281 (2002).
- S. Engen, B.-E. Sæther unpublished data.
- S. L. Pimm, *The Balance of Nature?* (Univ. of Chicago Press, Chicago, 1991).
- A. Ariño, S. L. Pimm, *Evol. Ecol.* **9**, 429 (1995).
- T. Coulson et al., *Science* **292**, 1528 (2001).
- O. N. Bjørnstad, B. T. Grenfell, *Science* **293**, 638 (2001).
- We thank H. Weimerskirch and A. Dhondt for access to unpublished data and R. Lande and R. Aanes for critically reading a previous draft. Supported by the Research Council of Norway, the EU Commission (project METABIRD), and a grant from Programme International Cooperation Scientifique (CNRS) to B.-E.S.

7 December 2001; accepted 21 January 2002

The RAR1 Interactor SGT1, an Essential Component of R Gene-Triggered Disease Resistance

Cristina Azevedo,^{1*} Ari Sadanandom,^{1*} Katsumi Kitagawa,² Andreas Freialdenhoven,³ Ken Shirasu,^{1†} Paul Schulze-Lefert^{1,3}

Plant disease resistance (R) genes trigger innate immune responses upon pathogen attack. RAR1 is an early convergence point in a signaling pathway engaged by multiple R genes. Here, we show that RAR1 interacts with plant orthologs of the yeast protein SGT1, an essential regulator in the cell cycle. Silencing the barley gene *Sgt1* reveals its role in R gene-triggered, *Rar1*-dependent disease resistance. SGT1 associates with SKP1 and CUL1, subunits of the SCF (Skp1-Cullin-F-box) ubiquitin ligase complex. Furthermore, the RAR1-SGT1 complex also interacts with two COP9 signalosome components. The interactions among RAR1, SGT1, SCF, and signalosome subunits indicate a link between disease resistance and ubiquitination.

Plant disease resistance (R) genes are key components in pathogen perception; R genes activate a battery of defense reactions, collectively called the hypersensitive response (HR) (1). A number of R genes from various plant species have been isolated and characterized in detail

(2). Although different R genes confer resistance to a variety of pests, including bacteria, viruses, fungi, nematodes, and insects, many R gene products share common structural modules such as a nucleotide-binding site and a leucine-rich repeat domain. The structural sim-